YEAST MEIOSIS

Sister kinetochores are mechanically fused during meiosis I in yeast

Krishna K. Sarangapani,[1]* Eris Duro,[2]* Yi Deng,[1] Flavia de Lima Alves,[2] Qiaozhen Ye,[3] Kwaku N. Opoku,[1] Steven Ceto,[4]† Juri Rappsilber,[2,5] Kevin D. Corbett,[3,6] Sue Biggins,[4,7] Adèle L. Marston,[2]‡ Charles L. Asbury[1]‡

Production of healthy gametes requires a reductional meiosis I division in which replicated sister chromatids comigrate, rather than separate as in mitosis or meiosis II. Fusion of sister kinetochores during meiosis I may underlie sister chromatid comigration in diverse organisms, but direct evidence for such fusion has been lacking. We used laser trapping and quantitative fluorescence microscopy to study native kinetochore particles isolated from yeast. Meiosis I kinetochores formed stronger attachments and carried more microtubule-binding elements than kinetochores isolated from cells in mitosis or meiosis II. The meiosis I–specific monopolin complex was both necessary and sufficient to drive these modifications. Thus, kinetochore fusion directs sister chromatid comigration, a conserved feature of meiosis that is fundamental to Mendelian inheritance.

The hallmark of meiosis is a twofold reduction in ploidy, which occurs because one round of DNA replication is followed by two rounds of chromosome segregation. Sister chromatids distinctly comigrate during meiosis I, thereby enabling segregation of homologous chromosomes. During meiosis II, which resembles mitosis, the sister chromatids separate (fig. S1, A and B). It has been suggested that the comigration of sister chromatids during meiosis I depends on fusion of sister kinetochores in a range of organisms (*1*–*4*) (fig. S1C). Because fused sister kinetochore pairs would contain more microtubule-binding elements than individual kinetochores, we reasoned that they might form stronger attachments to microtubules. Alternatively, if one kinetochore within each sister pair was selectively inactivated during meiosis I (*5*, *6*), then the remaining active kinetochores would probably form attachments with similar strength relative to individual mitotic and meiosis II kinetochores.

To distinguish between the "fusion" and "one-sister shut-off" mechanisms, we purified native kinetochore particles from yeast cells arrested in metaphase of meiosis I (via meiosis-specific depletion of Cdc20) (*7*), using methods developed for the isolation of mitotic particles (*8*, *9*). The purified material contained essentially all known kinetochore components (table S1), and its bulk composition was very similar to material isolated from mitosis (Fig. 1A; fig. S2, A and B; and table S1). We used fluorescence- and laser trap–based assays to determine whether the meiosis I kinetochore particles remained functional in vitro. As shown previously for mitotic particles (*8*), fluorescently labeled particles isolated from meiosis I cultures bound specifically to microtubules and tracked processively with disassembling microtubule tips (Fig. 1B and movie S1). Furthermore, meiosis I kinetochore particles formed load-bearing attachments to microtubule tips, supporting forces up to 15 pN and persisting through "catastrophe" and "rescue" events, in which the filament switched from assembly to disassembly and vice versa (Fig. 1C). Thus, native kinetochore particles isolated from meiotic cultures are functional. The meiotic particles formed very-long-lived tip attachments with a mean lifetime of 52 ± 23 min at 7 pN of tension, double the lifetime measured previously for mitotic particles (26 ± 6 min) at a similar level of tension (7.2 pN) (*8*).

The long lifetimes of attachments formed by meiosis I kinetochore particles suggested that they may be stronger than particles from mitotic cells. To assess their strength directly, we attached the meiosis I kinetochore particles to growing microtubule tips and tested them using a force ramp, where force was increased at a constant rate until the attachments ruptured (Fig. 1D). Control kinetochore particles isolated from metaphase-arrested mitotic cells ruptured at an average force of 9.4 ± 0.4 pN (Fig. 2B), which is indistinguishable from the strength of particles harvested during vegetative (asynchronous mitotic) growth (*8*). Rupture strengths were unaffected by differences in ploidy and were relatively insensitive to the method of mitotic cell cycle arrest (fig. S3). Meiosis I particles, however, formed significantly stronger attachments, rupturing at forces ranging from 6.5 to 22 pN (i.e., up to the load limit of our laser trap), with an average of 13.1 ± 0.3 pN (Fig. 2, A and B, and table S2). Mean rupture forces for both meiosis I and mitotic particles remained invariant as the density of particles on the beads was reduced below the single-particle limit (fig. S4), indicating that higher strength is an intrinsic property of individual meiosis I kinetochore particles.

To determine whether the higher kinetochore attachment strength is specific to meiosis I or persists into meiosis II, we prepared synchronized meiotic cultures by releasing cells from a prophase I block (*10*, *11*). Particles harvested from synchronized metaphase I cells formed attachments that ruptured at 13.1 ± 0.6 pN, on average (Fig. 2, A and B, meiosis I*). However, particles from synchronized metaphase II cells ruptured at 9.3 ± 0.7 pN, on average (Fig. 2, A and B, meiosis II*). Thus, the higher intrinsic strength of kinetochore particles occurs specifically during meiosis I and returns to mitotic-like levels as cells progress into meiosis II.

If the particles isolated from meiosis I cells are fused sister kinetochore pairs, they should contain more microtubule binding elements than mitotic particles. We purified fluorescent particles doubly tagged with SNAP-549 on Nuf2 (a subunit of the microtubule-binding Ndc80 complex) and CLIP-647 on Mif2 (an inner kinetochore component orthologous to CENP-C). Spore viability was unaffected, and rupture strengths for the fluorescent particles were indistinguishable from untagged particles (fig. S5 and table S2), indicating no loss of functionality. The purified kinetochore material contained a mixture of dual-color particles carrying both Nuf2 and Mif2, plus subcomplexes lacking Nuf2 or Mif2 (Fig. 2C). Subcomplexes with just one detectable Nuf2 [identifiable by their single-step photobleaching behavior (fig. S6)] served as internal controls, allowing normalization of particle brightnesses into estimates for the approximate numbers of Nuf2 molecules associated with each particle. Dual-color particles from meiosis I cells carried more Nuf2 molecules, on average [6.5 ± 2.8 (mean ± SD from N = 4 preparations)], than those from vegetatively growing cells, which had 3.8 ± 1.3 (N = 4) (Fig. 2, D and E). The apparent Nuf2 content was variable and lower than in vivo estimates [which suggest 8 to 20 copies per mitotic kinetochore (*12*, *13*)]. However, consistent with the fusion model, Nuf2 content was significantly higher for dual-color meiosis I particles than for vegetative particles prepared in tandem, by a factor of 1.66 ± 0.26 (mean ± SD, N = 4 tandem pairs; P = 0.014 by t test).

If fusion of sister kinetochore pairs underlies the increased strength of meiosis I kinetochore particles, the increase should vanish if the particles are harvested from cells in which every kinetochore lacks a sister. We engineered cells to undergo meiosis without replicating their DNA [via meiosis-specific depletion of Cdc6 (*14*), part of the prereplicative complex (*15*)]. Because the lack of sister chromatids precludes homology-based DNA repair (*16*), we also deleted the Spo11 endonuclease, thereby avoiding high levels of DNA damage that might interfere with meiotic progression. Spo11 catalyzes formation of the chiasmata that link homologous chromosomes

[1]Department of Physiology and Biophysics, University of Washington, Seattle, WA 98195, USA. [2]Wellcome Trust Centre for Cell Biology, University of Edinburgh, Edinburgh, UK. [3]Ludwig Institute for Cancer Research, San Diego Branch, La Jolla, CA 92093, USA. [4]Division of Basic Sciences, Fred Hutchinson Cancer Research Center, Seattle, WA 98109, USA. [5]Institute of Bioanalytics, Department of Biotechnology, Technische Universität Berlin, Berlin, Germany. [6]Department of Cellular and Molecular Medicine, University of California, San Diego, La Jolla, CA 92093, USA. [7]Department of Biochemistry, University of Washington, Seattle, WA 98195, USA.
*These authors contributed equally to this work. †Present address: Department of Neurosciences, University of California, San Diego, CA 92093, USA. ‡Corresponding author. E-mail: casbury@u.washington.edu (C.L.A.); adele.marston@ed.ac.uk (A.L.M.)

(*17*), so its deletion (*spo11*Δ) enabled us to test whether tension across homologs is required for sister kinetochore fusion (*18*). Kinetochore particles from *spo11*Δ cells were identical in strength to those from wild-type cells, indicating that linkage between homologs (and, thus, spindle-generated tension across them) was dispensable for the high attachment strength of meiosis I kinetochores (Fig. 2, A and B, *no chiasmata*).

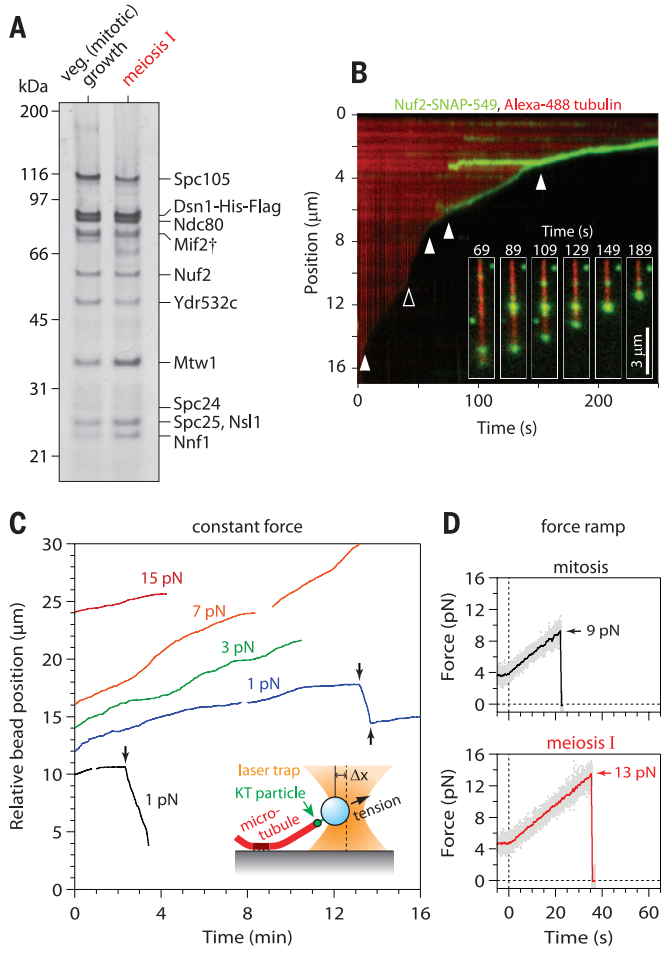

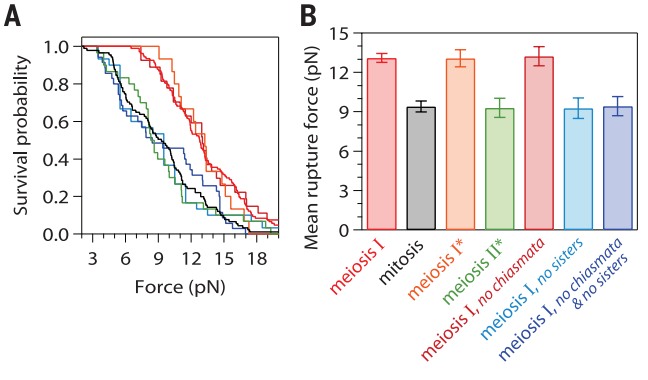

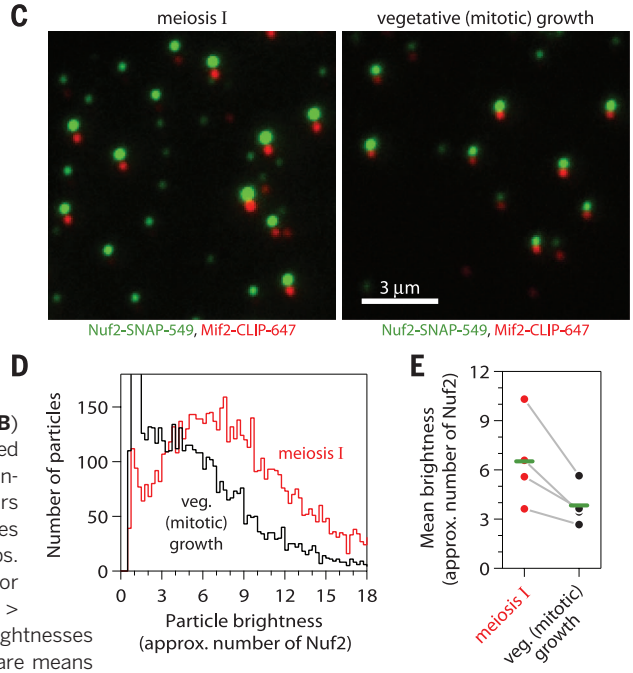

Fig. 1. Native kinetochore particles from meiotic cells recapitulate tip-coupling in vitro. (**A**) Core kinetochore proteins copurified from cells undergoing vegetative (mitotic) growth and cells arrested in metaphase I of meiosis, visualized by silver-stained SDS–polyacrylamide gel electrophoresis (*9*). Mif2 (†) comigrates with nonspecific background proteins (*8*). kDa, kilodaltons. (**B**) Kymograph showing movement of fluorescent meiosis I kinetochore particles (green) driven by a disassembling microtubule (red) (see movie S1). Filled arrowheads mark tip-particle encounters; the open arrowhead denotes particle release. Insets shows images at indicated times. (**C**) Position versus time for tip-attached meiosis I particles tested with a force clamp at indicated loads. Arrows mark catastrophes and rescue. Intervals when the laser trap was briefly shuttered (to clear debris) appear as gaps in the 1- and 7-pN traces. The inset shows a schematic of the assay (*9*). KT, kinetochore. (**D**) Tensile force versus time for indicated particles bound to assembling tips and tested with a 0.25–pN s^{-1} force ramp. Gray dots show raw data; colored traces show the same data after smoothing (500-ms sliding boxcar average). Dashed vertical lines mark the start of the force ramp. Arrows denote rupture.

Fig. 2. Meiosis I kinetochore particles are stronger and brighter. (**A** and **B**) Distributions of rupture force (A) and mean rupture force values (B) for indicated kinetochore particles (color-matched). Asterisks indicate particles from cells undergoing meiosis synchronized by release from a prophase I block. Error bars represent SEM (N = 15 to 107 ruptures). (**C**) Fluorescence images of particles carrying Nuf2-SNAP-549 (green) and Mif2-CLIP-647 (red) bound to coverslips. Colors are offset slightly; green-red pairs represent colocalized, dual-color particles. (**D**) Distributions of Nuf2 brightness for dual-color particles (N > 4900 particles) relative to the brightness of a single Nuf2. (**E**) Mean Nuf2 brightnesses for dual-color particles from four pairs of kinetochore preparations. Points are means from individual preparations. Gray lines connect means from particles prepared in tandem (*9*); green horizontal lines are means across all preparations.

However, high strength was lost when meiosis I particles were harvested from *cdc6-meiotic-null* cells (Fig. 2, A and B, *no sisters* or *no chiasmata & no sisters*). Thus, sister kinetochores are required for the increased strength of meiosis I kinetochore particles, as predicted by the fusion model.

The meiosis I–specific monopolin complex consists of four proteins (Mam1, Csm1, Lrs4, and Hrr25) (*5*, *19*–*21*) with twin kinetochore-binding sites that have been proposed to directly cross-link sister kinetochores in budding yeast (*1*, *5*, *20*, *22*). However, because the receptor for monopolin, Dsn1 (*1*, *23*), is present in multiple copies in the kinetochore (*12*), another possibility is that the twin monopolin sites bind to the same kinetochore and inactivate it, thereby shutting off one of the two sister kinetochores (fig. S1C) (*5*, *6*).

Monopolin was detectable at low levels in kinetochore material from meiosis I cultures (fig. S2C). To test the impact of monopolin on the behavior of kinetochore particles, we genetically disrupted its function in three ways (*mam1*Δ, *csm1-L161D*, and *dsn1-*Δ*N*), all of which disrupt sister comigration during meiosis I (*1*, *21*, *23*). In all cases, we found that the high 13-pN strength of meiosis I kinetochore particles was lost and their strength returned to mitosis-like levels (~9 pN) (Fig. 3), confirming that monopolin is required for high attachment strength. We also engineered cells to ectopically express monopolin during mitosis by inducing expression of *MAM1* together with *CDC5* (encoding Polo kinase), which caused erroneous co-orientation in 28% of cells (*5*). Kinetochore particles isolated from these cells gave a bimodal rupture force distribution (Fig. 3A) with an intermediate average strength of 11.2 ± 0.4 pN (Fig. 3B). This observation may be explained by the incomplete penetrance of monopolin induction in these cells (*5*).

To test whether kinetochores can be fused by monopolin in the absence of other cellular factors, we recombinantly expressed and purified the four-protein monopolin complex [containing a kinase-dead Lys^{38}→Arg^{38} mutant of Hrr25 (fig. S2D)] (*22*) and incubated it with isolated kinetochore particles. Incubation with recombinant monopolin was sufficient to strengthen mitotic particles and also particles from meiosis I cells in which monopolin was disrupted (*mam1*Δ or *csm1-L161D*), raising their mean rupture forces from ~9 to ~13 pN (Fig. 4, A and B) in a dose-dependent manner (Fig. 4C). However, the same treatment did not affect the strength of particles from cells lacking the monopolin binding site on Dsn1 (*dsn1-*Δ*N*) (Fig. 4, A and B). Likewise, monopolin addition did not strengthen particles (*mam1*Δ) prelinked to laser trapping beads (Fig. 4C), presumably because immobilization on beads prevented cross-linking of the particles. When fluorescent particles from vegetatively growing cells were incubated with increasing amounts of monopolin, their average brightness grew monotonically, and the approximate number of Nuf2 molecules associated with each particle increased twofold, from 4.8 ± 0.4 to 10.9 ± 1.5 (mean ± SD, $N \geq 2$ experiments) (Fig. 4D). Thus, monopolin alone is sufficient for fusion of kinetochore particles in vitro.

Sister chromatid comigration is a universal feature of meiosis I that governs Mendelian inheritance, and its failure is a major cause of birth defects and infertility (*24*). Here we have shown

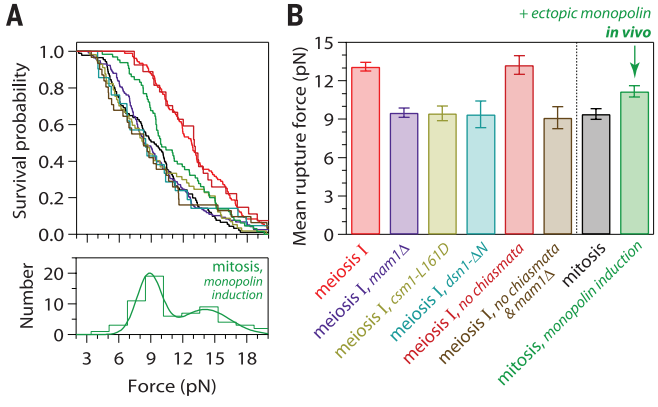

Fig. 3. Monopolin is necessary for the high strength of meiosis I kinetochore particles and is sufficient in vivo. (**A** and **B**) Distributions of rupture force (A) and mean rupture force values (B) for indicated kinetochore particles (color-matched). Data for particles from meiosis I (red), meiosis I without chiasmata (dark red), and mitosis (black) are replotted from Fig. 2, A and B, for comparison. Error bars represent SEM (N = 21 to 118 ruptures).

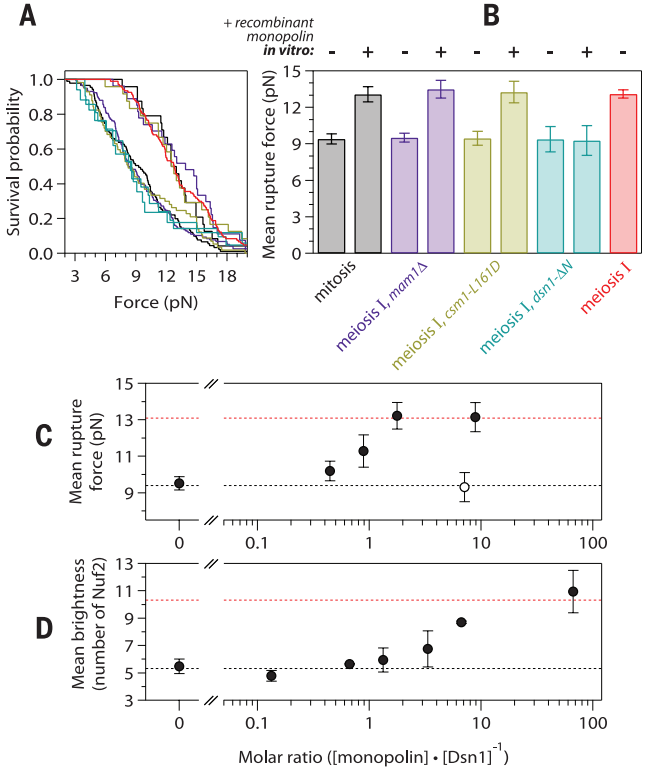

Fig. 4. Pure recombinant monopolin is sufficient to increase the strength and brightness of kinetochore particles in vitro. (**A** and **B**) Distributions of rupture force (A) and mean rupture force values (B) for kinetochore particles (color-matched) after incubation with recombinant monopolin [at molar ratio 1.8 versus Dsn1-His-Flag; "+" in (B)]. Data for particles without monopolin incubation ["-" in (B)] are replotted from Fig. 3, A and B, for comparison. Error bars represent SEM (N = 17 to 118 ruptures). (**C**) Mean rupture forces for meiosis I, *mam1*Δ kinetochore particles after incubation with indicated amounts of recombinant monopolin (*9*). Filled circles are data from particles preincubated with monopolin before linking to polystyrene laser trapping beads. The open circle shows control in which particles were first linked to trapping beads and subsequently incubated with monopolin. Error bars represent SEM (N = 28 to 118 ruptures). Dashed lines denote means for mitosis (black) and meiosis I (red) particles (from Fig. 2B). (**D**) Mean Nuf2 brightnesses for dual-color particles isolated from cells undergoing vegetative (mitotic) growth, incubated with indicated amounts of recombinant monopolin. Error bars represent SD (N = 2 or 3 experiments). Dashed lines represent mean brightnesses for dual-color vegetative (black) and meiosis I (red) kinetochore particles prepared on the same day, without monopolin incubation (from Fig. 2E).

that a meiosis I–specific factor from budding yeast, monopolin, generates kinetochores with more microtubule-binding elements and greater strength. These findings provide direct evidence that sister kinetochore fusion underlies the cosegregation of sister chromatids during meiosis I.

REFERENCES AND NOTES

1. K. D. Corbett *et al*., *Cell* **142**, 556–567 (2010).
2. X. Li, R. K. Dawe, *Nat. Cell Biol.* **11**, 1103–1108 (2009).
3. L. S. Goldstein, *Cell* **25**, 591–602 (1981).
4. L. V. Paliulis, R. B. Nicklas, *J. Cell Biol.* **150**, 1223–1232 (2000).
5. F. Monje-Casas, V. R. Prabhu, B. H. Lee, M. Boselli, A. Amon, *Cell* **128**, 477–490 (2007).
6. M. Winey, G. P. Morgan, P. D. Straight, T. H. Giddings Jr., D. N. Mastronarde, *Mol. Biol. Cell* **16**, 1178–1188 (2005).
7. B. H. Lee, A. Amon, *Science* **300**, 482–486 (2003).
8. B. Akiyoshi *et al*., *Nature* **468**, 576–579 (2010).
9. Materials and methods are available as supplementary materials on *Science* Online.
10. T. M. Carlile, A. Amon, *Cell* **133**, 280–291 (2008).
11. K. R. Benjamin, C. Zhang, K. M. Shokat, I. Herskowitz, *Genes Dev.* **17**, 1524–1539 (2003).
12. A. P. Joglekar, D. C. Bouck, J. N. Molk, K. S. Bloom, E. D. Salmon, *Nat. Cell Biol.* **8**, 581–585 (2006).
13. J. Lawrimore, K. S. Bloom, E. D. Salmon, *J. Cell Biol.* **195**, 573–582 (2011).
14. A. Hochwagen, W. H. Tham, G. A. Brar, A. Amon, *Cell* **122**, 861–873 (2005).
15. J. H. Cocker, S. Piatti, C. Santocanale, K. Nasmyth, J. F. Diffley, *Nature* **379**, 180–182 (1996).
16. T. Goldfarb, M. Lichten, *PLOS Biol.* **8**, e1000520 (2010).
17. S. Keeney, C. N. Giroux, N. Kleckner, *Cell* **88**, 375–384 (1997).
18. M. A. Shonn, R. McCarroll, A. W. Murray, *Science* **289**, 300–303 (2000).
19. M. Petronczki *et al*., *Cell* **126**, 1049–1064 (2006).
20. K. P. Rabitsch *et al*., *Dev. Cell* **4**, 535–548 (2003).
21. A. Tóth *et al*., *Cell* **103**, 1155–1168 (2000).
22. K. D. Corbett, S. C. Harrison, *Cell Reports* **1**, 583–589 (2012).
23. S. Sarkar *et al*., *PLOS Genet.* **9**, e1003610 (2013).
24. K. T. Jones, S. I. Lane, *Development* **140**, 3719–3730 (2013).

ACKNOWLEDGMENTS

We thank A. Hoskins, M. Miller, N. Umbreit, and E. Yusko for helpful comments. We thank A. Desai for providing antibodies and A. Hoskins for SNAPf and CLIPf plasmids. The Wellcome Trust supported this work through a Sir Henry Wellcome Fellowship to E.D. (096078), Senior Research Fellowships to A.L.M. (090903) and J.R. (084229), and two Wellcome Trust Centre Core Grants (077707 and 092076) and an instrument grant (091020). The work was also supported by NIH grants to C.L.A. (RO1GM079373 and S10RR026406), S.B. (R01GM064386), and K.D.C. (R01GM104141) and by a Packard Fellowship to C.L.A. (2006-30521). K.D.C. also acknowledges support from the Ludwig Institute for Cancer Research and the Sidney Kimmel Foundation. Additional data described in this work can be found in the supplementary materials. E.D., K.K.S., S.B., A.L.M., and C.L.A. conceived the experiments. E.D. generated new yeast strains and isolated kinetochore particles. K.K.S. performed laser trap experiments. Y.D. performed the fluorescence measurements. F.d.L.A. and J.R. performed proteomics analysis. Q.Y. and K.D.C. purified monopolin. K.N.O. and S.C. optimized fluorescent labeling of kinetochore particles. E.D., K.K.S., A.L.M., and C.L.A. prepared the manuscript.

SUPPLEMENTARY MATERIALS

www.sciencemag.org/content/346/6206/248/suppl/DC1
Materials and Methods
Figs. S1 to S8
Tables S1 to S3
References (*25*–*42*)
Movie S1
Additional Data Tables S1 to S3

30 May 2014; accepted 1 September 2014
Published online 11 September 2014;
10.1126/science.1256729

LUNG CANCER EVOLUTION

Spatial and temporal diversity in genomic instability processes defines lung cancer evolution

Elza C. de Bruin,[1]* Nicholas McGranahan,[2,3]* Richard Mitter,[2]* Max Salm,[2]* David C. Wedge,[4]* Lucy Yates,[4,5]† Mariam Jamal-Hanjani,[1]† Seema Shafi,[1] Nirupa Murugaesu,[1] Andrew J. Rowan,[2] Eva Grönroos,[2] Madiha A. Muhammad,[1] Stuart Horswell,[2] Marco Gerlinger,[2] Ignacio Varela,[6] David Jones,[4] John Marshall,[4] Thierry Voet,[4,7] Peter Van Loo,[4,7] Doris M. Rassl,[8] Robert C. Rintoul,[8] Sam M. Janes,[9] Siow-Ming Lee,[1,10] Martin Forster,[1,10] Tanya Ahmad,[10] David Lawrence,[10] Mary Falzon,[10] Arrigo Capitanio,[10] Timothy T. Harkins,[11] Clarence C. Lee,[11] Warren Tom,[11] Enock Teefe,[11] Shann-Ching Chen,[11] Sharmin Begum,[2] Adam Rabinowitz,[2] Benjamin Phillimore,[2] Bradley Spencer-Dene,[2] Gordon Stamp,[2] Zoltan Szallasi,[12,13] Nik Matthews,[2] Aengus Stewart,[2] Peter Campbell,[4] Charles Swanton[1,2]‡

Spatial and temporal dissection of the genomic changes occurring during the evolution of human non–small cell lung cancer (NSCLC) may help elucidate the basis for its dismal prognosis. We sequenced 25 spatially distinct regions from seven operable NSCLCs and found evidence of branched evolution, with driver mutations arising before and after subclonal diversification. There was pronounced intratumor heterogeneity in copy number alterations, translocations, and mutations associated with APOBEC cytidine deaminase activity. Despite maintained carcinogen exposure, tumors from smokers showed a relative decrease in smoking-related mutations over time, accompanied by an increase in APOBEC-associated mutations. In tumors from former smokers, genome-doubling occurred within a smoking-signature context before subclonal diversification, which suggested that a long period of tumor latency had preceded clinical detection. The regionally separated driver mutations, coupled with the relentless and heterogeneous nature of the genome instability processes, are likely to confound treatment success in NSCLC.

Lung cancer is the leading cause of cancer-related mortality (*1*, *2*). Understanding the pathogenesis and evolution of lung cancer may lead to greater insight into tumor initiation and maintenance and may guide therapeutic interventions. Previous work characterizing the genome of non–small cell lung cancer (NSCLC) has demonstrated that NSCLC genomes exhibit hundreds of nonsilent mutations together with copy number aberrations and genome doublings (*3*–*9*). Although subclonal populations have been identified within single biopsies (*9*), the extent of genomic diversity within primary NSCLCs remains unclear. Moreover, although both exogenous mutational processes, such as smoking (*10*–*12*), and endogenous processes, such as up-regulation of APOBEC cytidine deaminases (*13*–*15*), have been found to contribute to the large mutational burden in NSCLC, the temporal dynamics of these processes and their contribution to driver somatic aberrations over time remain unknown.

To investigate lung cancer evolution, we performed multiregion whole-exome and/or whole-genome sequencing (M-seq WES/WGS) on a total of 25 tumor regions, collected from seven NSCLC patients who underwent surgical resection before receiving adjuvant therapy. The major NSCLC histological subtypes, including adenocarcinoma (LUAD) and squamous cell carcinoma (LUSC), were represented (table S1). Sequencing of tumor and normal DNA to mean coverage depths of 107× and 54× for M-seq WES and M-seq WGS, respectively (table S2), identified 1884 nonsilent and 76,129 silent mutations (*16*).

To evaluate the intratumor heterogeneity of nonsilent mutations, we classified each mutation as ubiquitous (present in all tumor regions) or heterogeneous (present in at least one, but not all, regions). Spatial intratumor heterogeneity was identified in all seven NSCLCs, with a median of 30% heterogeneous mutations (range 4

[1]Cancer Research UK Lung Cancer Centre of Excellence, University College London Cancer Institute, London WC1E 6BT, UK. [2]Cancer Research UK London Research Institute, London WC2A 3LY, UK. [3]Centre for Mathematics and Physics in the Life Science and Experimental Biology (CoMPLEX), University College London, London WC1E 6BT, UK. [4]Wellcome Trust Sanger Institute, Hinxton, CB10 1SA, UK. [5]University of Cambridge, Cambridge CB2 1TN, UK. [6]Instituto de Biomedicina y Biotecnología de Cantabria (CSIC-UC-Sodercan), Departamento de Biología Molecular, Universidad de Cantabria, Santander, Spain. [7]Department of Human Genetics, University of Leuven, 3000 Leuven, Belgium. [8]Papworth Hospital NHS Foundation Trust, Cambridge CB23 3RE, UK. [9]Lungs for Living Research Centre, University College London, London WC1E 6BT, UK. [10]University College London Hospitals, London NW1 2BU, UK. [11]Thermo Fisher Scientific, Carlsbad, CA 92008, USA. [12]Technical University of Denmark, 2800 Kongens Lyngby, Denmark. [13]Children's Hospital Informatics Program, Harvard Medical School, Boston, MA 02115, USA.
*These authors contributed equally to this work. †These authors contributed equally to this work. ‡**Corresponding author. E-mail: charles.swanton@cancer.org.uk**

Editor's Summary

Monopolin masterfully manages meiosis

Biologists have wondered for decades how replicated sister chromatids, which normally separate during mitotic cell division, instead comigrate during the first meiotic division, meiosis I. This process segregates chromosomal homologs and is needed to produce haploid gametes after the second, more mitosis-like, meiotic division. One hypothesis for sister chromatid comigration suggests that meiosis I–specific factors directly cross-link the sister kinetochores that attach each sister chromatid to dynamic microtubule tips. Yeast possesses a putative kinetochore cross-linker, known as monopolin, but monopolin's precise role during meiosis I is unknown. Sarangapani *et al.* isolated functional meiotic kinetochores from yeast cells. They reconstituted kinetochore activity in vitro and found that monopolin causes kinetochore fusion and underlies the sister chromatid comigration seen in meiosis I.

Science, this issue p. 248